



# Low-temperature electrochemical codeposition of aluminum-neodymium alloy in a highly stable solvate ionic liquid

Baoguo Zhang<sup>1,2</sup> · Zhongning Shi<sup>1,2</sup> · Lingling Shen<sup>1,2</sup> · Xiaozhen Liu<sup>1,2</sup> · Junli Xu<sup>3</sup> · Zhaowen Wang<sup>1,2</sup>

Received: 29 November 2018 / Revised: 14 March 2019 / Accepted: 10 April 2019 / Published online: 14 May 2019  
© Springer-Verlag GmbH Germany, part of Springer Nature 2019

## Abstract

A highly stable solvate ionic liquid comprising a 2:1 (mol/mol) mixture of ethylene carbonate (EC) and  $\text{AlCl}_3$  was used for near room-temperature electrochemical codeposition of an Al-Nd alloy using chlorides as precursors. This liquid is low-cost, easy to prepare, and has high electrochemical stability. The ionic structure was analyzed by  $^{27}\text{Al}$  nuclear magnetic resonance; Raman spectroscopy and the dissolution phenomenon was studied by ultraviolet-visible spectroscopy. The dissolution mechanism of  $\text{NdCl}_3$  in this solvate ionic liquid was derived as  $3[\text{AlCl}_2(\text{EC})_n]^+ + 2\text{NdCl}_3 \rightleftharpoons 2\text{Nd(III)} + 3[\text{AlCl}_4]^- + 3n\text{EC}$ . Cyclic voltammetry was used to explore the electrochemical behavior of Nd- and Al-containing species, revealing that the reduction of Al and Nd are both one-step electron-gaining processes. X-ray diffraction confirmed that an Al-Nd alloy can be obtained in the form of thermally stable  $\text{Al}_2\text{Nd}$  by potentiostatic electrolysis at high cathode overpotential ( $-3.5$  V vs. Al). Although the deposited alloy layer is not dense, Al-containing solvate ILs have immense potential in green electrometallurgy because of their higher tunability and similar properties to ILs.

**Keywords** Codeposition · Al-containing solvate ionic liquid · Dissolution mechanism · Al-Nd alloy

## Introduction

Alloys and compounds containing the rare-earth (RE) element Nd have received considerable attention due to their applications in high-performance magnets, glass lasers, aerospace materials, and other areas [1–3]. Particularly, the addition of Nd is an effective way to enhance the strength and improve the corrosion resistance of alloys by grain refinement [4].

The simplicity and flexibility of electrodeposition make it an effective method for extracting primary Nd and its alloys [5, 6]. Unfortunately, electrodeposition of Nd and its alloys in aqueous solutions is quite difficult to achieve because of its

negative deposition potential and high reactivity with water [7, 8]. As is known, the electrochemical reduction of RE metals is a relatively poorly studied problem, let alone Nd. From a practical viewpoint, electrodeposition of Nd-containing alloys is a more significance task compared to the electrodeposition of pure metals [9]. However, the preparation of Nd metal or Nd-containing alloys is conventionally performed by high-temperature molten salt electrolysis, which requires highly corrosive materials and consumes a large amount of energy [10–13]. In addition, organic solvents have been used as the support electrolyte for the electrodeposition of RE metals; however, they were found to be unsuitable due to their high volatility and low solubility of RE salts [14]. Therefore, the combination of high-solubility RE salts and a stable supporting electrolyte system is the key to making the low-temperature production of Nd and its alloys more energy-efficient and economical.

The development of ionic liquids (ILs) provides new possibilities for the electrodeposition of RE metals and Nd-containing alloys. ILs, originally well-known as room-temperature molten salts, have enormous potential applications in green electrometallurgy due to advantages such as their low vapor pressure, wide electrochemical window, and their ability to dissolve metallic species [15–17]. The

✉ Zhongning Shi  
znshi@mail.neu.edu.cn

<sup>1</sup> School of Metallurgy, Northeastern University, Shenyang 110819, People's Republic of China

<sup>2</sup> Key Laboratory for Ecological Metallurgy of Multimetallic Mineral (Ministry of Education), Shenyang 110819, People's Republic of China

<sup>3</sup> College of Science, Northeastern University, Shenyang 110819, People's Republic of China

electrodeposition of RE elements previously reported has been mainly investigated using four different families of ILs based on their cations. In particular, phosphonium, ammonium, pyrrolidinium, and imidazolium-based ILs have been studied with a variety of anions [18, 19]. Among them, however, only limited studies have been reported on neodymium electrodeposition. Kondo et al. researched the suitability of recovering Nd metal from triethyl-pentyl-phosphonium bis (trifluoromethyl-sulfonyl) amide ([P2225][TFSA]) [20] and Ota et al. studied the electrodeposition behavior of Nd (III) at elevated temperatures in this same IL, which has a wide electrochemical window and good thermal stability [21]. Matsumiya et al. studied the diffusion behavior and nucleation mechanisms of Nd complexes in the ionic liquid N,N-diethyl-N-methyl-N-(2-methoxyethyl) ammonium bis (trifluoromethyl-sulfonyl) amide [DEME][TFSA] using Nd (TFSA)<sub>3</sub> as a raw material [22]. Unfortunately, from a practical standpoint, the synthesis of these ILs is complex and the production cost of the Nd precursors is high, preventing their use in electrometallurgy at present.

IL-like systems have similar properties and characteristics to ILs, and are widely recognized as deep eutectic solvents (DESs) [23, 24] and liquid coordination complexes (LCCs) [25, 26], and have found extensive applications in metal extraction and catalytic synthesis due to their advantages such as low cost, ease of preparation, and biodegradability, among others. Against this backdrop, chloroaluminate IL-like systems, prepared by combining the Lewis acid AlCl<sub>3</sub> with Lewis base donor molecules, have attracted significant research attention due to their tunable Lewis acidity and high solubility [27, 28]. Thus far, a limited number of Lewis base donor molecules have been reported such as 4-propylpyridine [29], dipropyl sulphide [30], urea [31], and other amide species [32]. However, these molecules lack electrochemical stability and hence have only been proposed for aluminum electrodeposition [33], and are not considered suitable for the electrodeposition of RE metals. Regardless, their importance as soft materials in their own right has become more and more recognized [25]. Therefore, the discovery of new and stable ligands to extend the family of IL-like systems for practical applications in various fields is of great significance.

Recently, we described a novel Al-containing solvate IL with high electrochemical stability and used it for electrodeposition of Al, Al-Li alloys, and Li under ambient conditions [34]. Moreover, we reported that direct electrochemical deposition of lithium from lithium oxide can be achieved in this system [35]. The newly developed Al-containing solvate IL has the advantages of low cost, high tuneability, and similar benefits as ILs and exhibits excellent ability to dissolve metal chlorides. Tentatively, in this work, a stable and homogeneous IL-like system of chloroaluminate was formed between an O-donor, ethylene carbonate (EC), and a Lewis acid, AlCl<sub>3</sub>, at a molar ratio of 2:1 and applied to the electrodeposition of an

Al-Nd alloy using NdCl<sub>3</sub> as a Nd source. The dissolution mechanism of NdCl<sub>3</sub> in this solvate IL was studied using instrument technology, and the codeposition mechanism of an Al-Nd alloy was explored using cyclic voltammetry. Finally, the deposited material was confirmed and characterized by using X-ray diffraction (XRD) and scanning electron microscopy (SEM). We expect that our findings can make a contribution to the electrochemical reduction of Al-based active metal alloys, especially Al-based rare earth alloys at relatively low temperature.

## Experimental

### Preparation and characterization of electrolyte system

The reagents EC (99.0% purity), acetamide (AcA, 99.9% purity), LiCF<sub>3</sub>SO<sub>3</sub> (99.9% purity), anhydrous AlCl<sub>3</sub> (99.9% purity), and NdCl<sub>3</sub> (99.9% purity) were purchased from Shanghai Aladdin Biochemical Polytron Technologies Inc. and used directly without any purification. The IL-like system was synthesized by slowly adding a calculated amount of AlCl<sub>3</sub> into EC and AcA in a sample cell without external heating under a high-purity argon atmosphere in a glove box (MBRAUN MB 200B, Germany), where both the water and oxygen contents were maintained below 0.1 ppm. The homogeneous, transparent, colorless (slightly yellow under fluorescent light), and free-flowing EC/AlCl<sub>3</sub> (2:1, mole ratio) IL-like system was formed under continuous stirring for 4 h. The EC/AlCl<sub>3</sub> (2:1, mole ratio) IL-like system containing 4 mol% NdCl<sub>3</sub> was formed under continuous stirring for 6 h at 323 K. Raman spectra were recorded at room temperature using a LabRAM XploRA Raman spectrometer (Horiba Jobin Yvon, France) equipped with a 785-nm laser. <sup>27</sup>Al nuclear magnetic resonance (NMR) analysis of the IL-like system was described in our previous publication [34]. The absorption spectra of Nd (III) in the RTIL was measured by ultraviolet-visible (UV-vis) spectrometer (Perkin Elmer, Lambda750).

### Electrochemical analyses and characterization of deposits

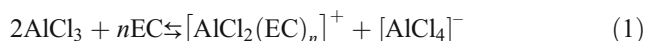
All electrochemical studies were performed using a PARSTAT 4000 (Princeton Applied Research, USA) electrochemical workstation controlled by the VersaStudio software with a three-electrode system. A tungsten wire (area = 0.24 cm<sup>2</sup>, 99.9%) working electrode, platinum wire (1 mm radius, 99.99%) counter electrode, and an Al wire (1 mm radius, 99.95%) reference electrode were used for the electrochemical studies. The tungsten working electrode was polished successively with increasingly finer grades of emery paper, washed with deionized water, and air-dried.

In the potentiostatic electrodeposition experiments, Al sheets (area = 1 cm<sup>2</sup>, 99.99%) were used as the cathode substrate, which was previously polished with SiC paper and then cleaned by sonication in ethanol. Surface morphologies of the deposits were visualized using SEM (Shimadzu SSX-550, Japan). The chemical composition of as-prepared deposits was characterized by energy-dispersive X-ray (EDX) spectroscopy attached to SEM. The phase compositions of the deposits were analyzed by XRD (PANalytical MPDDY 2094, Netherlands) using the Cu K $\alpha$  line (40 kV, 40 mA). Rapid determination of total porosities of the deposited materials was implemented by mercury intrusion porosimetry using an automatic mercury porosimeter (AutoPore V, Micromeritics Instruments Corp.)

## Results and discussion

### Structure of EC/AlCl<sub>3</sub> (2:1, mol/mol) and dissolution mechanism of NdCl<sub>3</sub> in EC/AlCl<sub>3</sub> (2:1, mol/mol)

Previous reports of chloroaluminate IL-like systems based on complexes of neutral ligands with AlCl<sub>3</sub> demonstrated that the asymmetric cleavage of AlCl<sub>3</sub> generated [AlCl<sub>2</sub>]<sup>+</sup> and [AlCl<sub>4</sub>]<sup>-</sup> ions (Eq. 1) [30, 31, 36]. Being strongly Lewis-acidic, [AlCl<sub>2</sub>]<sup>+</sup> cations cannot exist in an isolated form and interact with EC:



Raman spectra, shown in Fig. 1, indicate that the EC/AlCl<sub>3</sub> system with a mole ratio of 2:1 contains [AlCl<sub>4</sub>]<sup>-</sup> anions. However, no Lewis acid anions [Al<sub>2</sub>Cl<sub>7</sub>]<sup>-</sup> were observed near the corresponding characteristic Raman shift. In order to clarify the structure of the system, <sup>27</sup>Al NMR spectrum contrastive study of EC/AlCl<sub>3</sub> (2:1, mol/mol) solvate IL and AcA/AlCl<sub>3</sub> (1:1.2, mol/mol) liquid coordination complex was conducted.

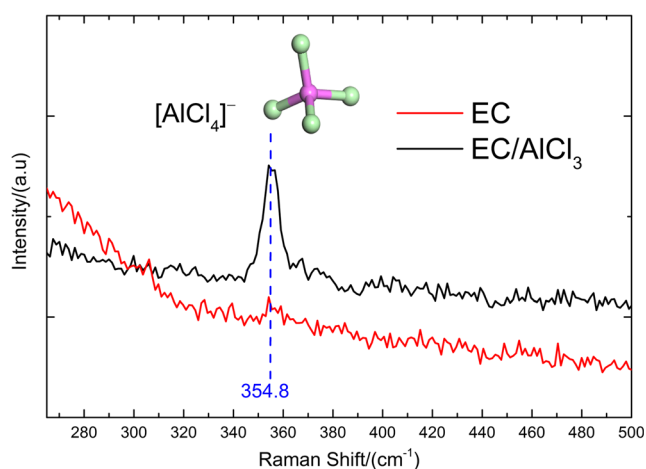


**Fig. 1** Raman spectra of EC and EC/AlCl<sub>3</sub> (2:1, mol/mol) at 298 K

Two clear peaks were observed from the black line in Fig. 2, indicating the existence of two major Al species. Six-coordinated Al species [AlCl<sub>2</sub>(EC)<sub>4</sub>]<sup>+</sup> was observed in the EC/AlCl<sub>3</sub> system with a large mole ratio of 2:1. Unfortunately, AlCl<sub>3</sub> cannot be dissolved in EC up to concentration greater than 50 mol%. However, AcA can dissolve AlCl<sub>3</sub> to large amounts of AlCl<sub>3</sub> (> 50 mol%) due to their diverse Lewis-acidic species. As shown in Fig. 2, it contains three main peaks, corresponding to four-coordinated cations [AlCl<sub>2</sub>(AcA)<sub>2</sub>]<sup>+</sup>, five-coordinated neutral molecules [AlCl<sub>3</sub>(AcA)<sub>2</sub>], and three potentially coexisting species: [Al<sub>2</sub>Cl<sub>7</sub>]<sup>-</sup>, [AlCl<sub>3</sub>(AcA)], and [Al<sub>2</sub>Cl<sub>6</sub>(AcA)]. This comparison study shows that the content of AlCl<sub>3</sub> has a great influence on the species of the AlCl<sub>3</sub>-based binary system. Therefore, the discovery of new and stable ligands to extend the family of IL-like systems for practical applications in various fields depends on the intrinsic properties of the molecular solvent itself.

Anyway, complex cationic species in the form of [AlCl<sub>2</sub>(base)<sub>n</sub>]<sup>+</sup> have been increasingly demonstrated by using multinuclear nuclear magnetic resonance spectroscopy in different AlCl<sub>3</sub>-based binary system. NdCl<sub>3</sub> can be dissolved in the above AcA/AlCl<sub>3</sub> liquid coordination complex from the experimental operation. However, it can also be dissolved in the binary AlCl<sub>3</sub>/EC system. Figure 3 shows the digital photo of EC/AlCl<sub>3</sub> before and after adding NdCl<sub>3</sub> under fluorescent lamp. The purple-red liquid was obtained after the addition of NdCl<sub>3</sub>. In order to confirm the dissolution phenomenon, UV-vis spectra comparative analysis was implemented (Fig. 4). Obviously, two absorption peak signals occur after adding 4 mol% NdCl<sub>3</sub>, which ascribes to the intraconfigurational transitions within 4f<sup>3</sup> shell of Nd (III). The most intense transition in the absorption spectrum at 580 nm and 747 nm are respectively <sup>4</sup>I<sub>9/2</sub> → <sup>2</sup>G<sub>7/2</sub> and <sup>4</sup>I<sub>9/2</sub> → <sup>4</sup>F<sub>7/2</sub> transition, which showed a pronounced fine structure [20]. Other common absorption peaks near ultraviolet region are related to the internal structure of EC and AlCl<sub>3</sub> themselves.

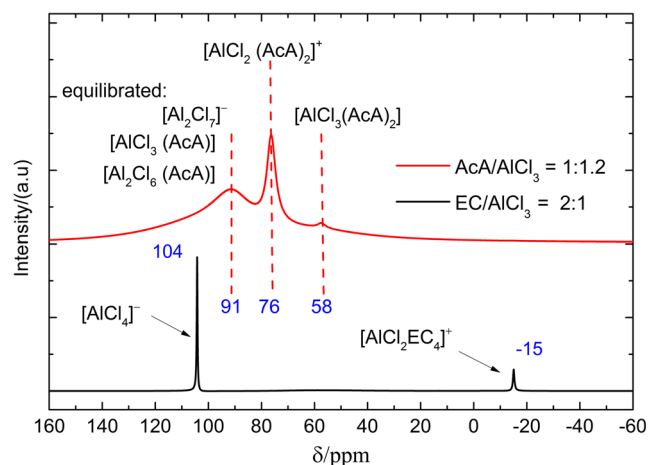


**Fig. 2** <sup>27</sup>Al NMR spectrum of EC/AlCl<sub>3</sub> (2:1, mol/mol) solvate IL and AcA/AlCl<sub>3</sub> (1:1.2, mol/mol) liquid coordination complex

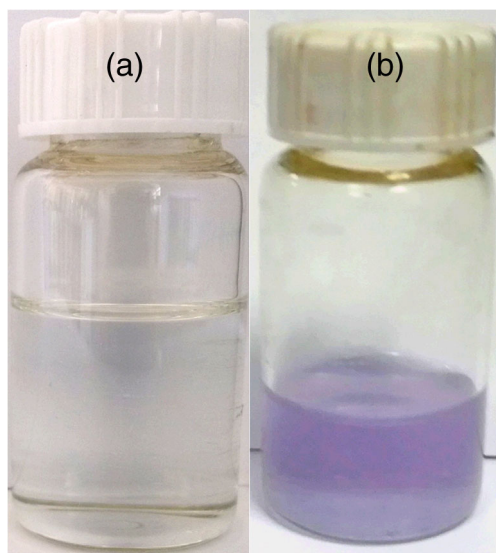
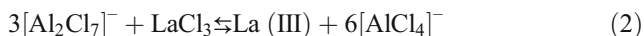


**Fig. 3** **a** EC/AlCl<sub>3</sub> (2:1, mole ratio) solvate IL at 323 K and **b** EC/AlCl<sub>3</sub> (2:1, mole ratio) solvate IL containing 4 mol% NdCl<sub>3</sub> under fluorescent lamp (excitation wavelength, 400–750 nm)

Based on the results of a study by Tsuda and co-workers [37], the dissolution reaction in the acidic AlCl<sub>3</sub>–1-ethyl-3-methylimidazolium chloride (AlCl<sub>3</sub>–EMICl) is thought to be (Eq. 2):



However, the dissolution mechanism of NdCl<sub>3</sub> can also be derived from the Lewis acidity of [AlCl<sub>2</sub>(EC)<sub>n</sub>]<sup>+</sup> as follows (Eq. 3):



Combining Eq. 1–3, Eq. 4 can be obtained:

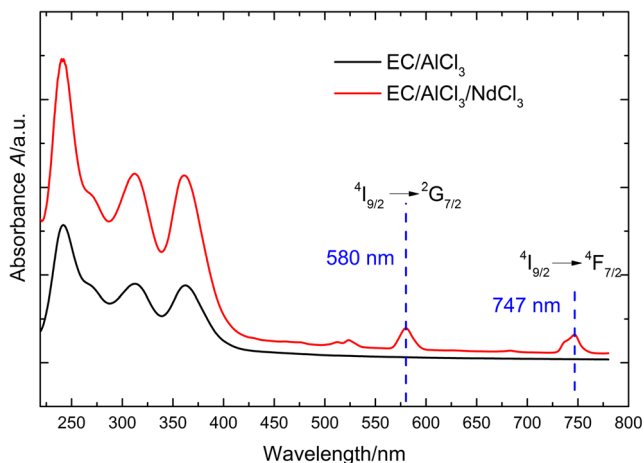
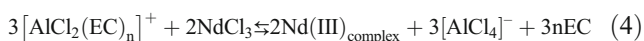


**Fig. 4** UV-vis spectra comparative analysis between EC/AlCl<sub>3</sub> (2:1, mole ratio) solvate IL and EC/AlCl<sub>3</sub> (2:1, mole ratio) solvate IL containing 4 mol% NdCl<sub>3</sub> at 323 K

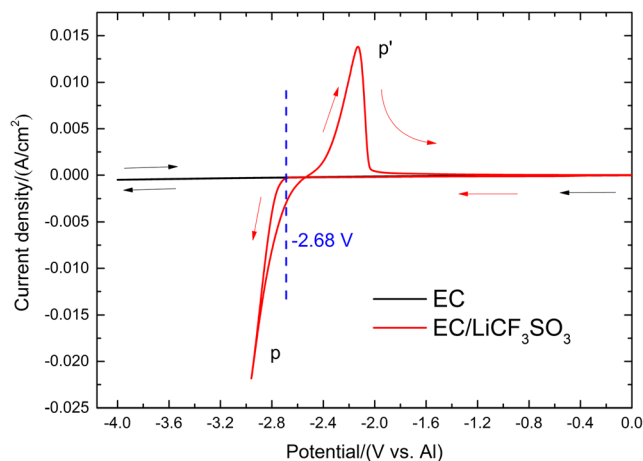


**Fig. 5** CV curve of neat EC and EC containing 4 mol% LiCF<sub>3</sub>SO<sub>3</sub> recorded at 313 K, at a scan rate of 50 mV/s, start point 0 V vs. Al

This suggests that the solubility of NdCl<sub>3</sub> depends on the amount of [AlCl<sub>2</sub>]<sup>+</sup> cations in the liquid. According to the above analysis, the highest solubility of NdCl<sub>3</sub> in this EC/AlCl<sub>3</sub> (2:1, mole ratio) solvate IL can theoretically be as high as 10 mol%. Unfortunately, this cannot be achieved in practice. In addition, the [AlCl<sub>2</sub>]<sup>+</sup> cation has never been reported in the literature, and no direct spectroscopic evidence of its existence has ever been presented [38].

Furthermore, charge-neutral complexes such as [AlCl<sub>3</sub>(base)<sub>2</sub>] also exist in the liquid, which occupy a part of the Lewis acid AlCl<sub>3</sub> [34]. Therefore, the ideal solubility of NdCl<sub>3</sub> is difficult to reach. Regardless, the discovery of the [AlCl<sub>2</sub>]<sup>+</sup> cation and confirmation of its existence are thus of great scientific significance [34].

### Cyclic voltammetry and potentiostatic deposition

EC is a polar aprotic solvent with low volatility, excellent chemical compatibility, and significant solubilizing power, which is often used as a high-permittivity component of

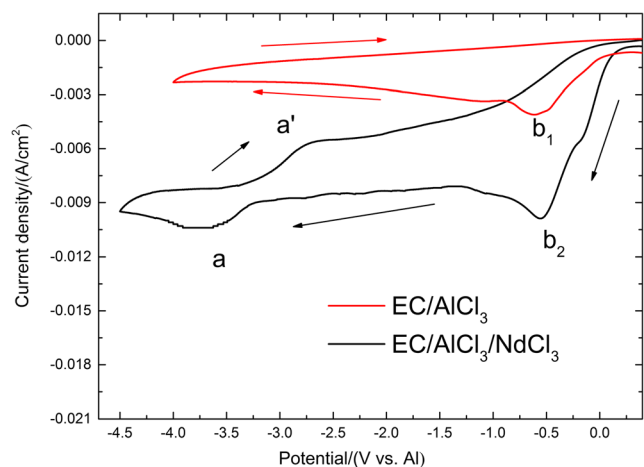


**Fig. 6** CV curve of EC/AlCl<sub>3</sub> (2:1, mole ratio) solvate IL before and after containing 4 mol% NdCl<sub>3</sub> recorded at 323 K, at a scan rate of 50 mV/s

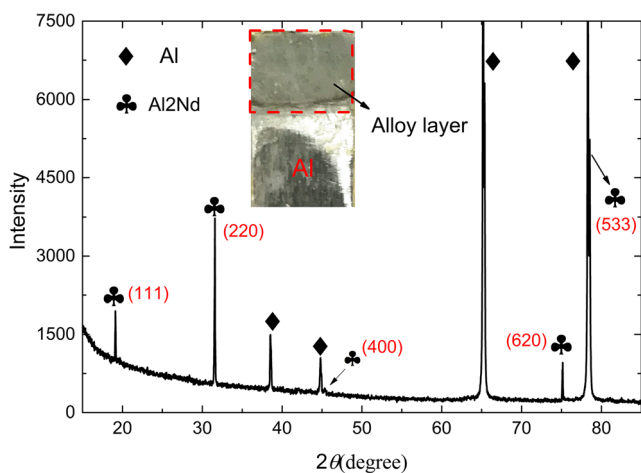


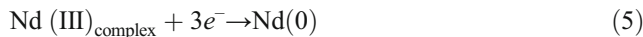
**Fig. 7** XRD pattern of the material deposited on the high-purity aluminum sheet. The inset is a digital photo

electrolytes in lithium-ion batteries. The cyclic voltammograms of EC show an excellent ability to withstand voltage due to its high dielectrical property, and the cathode limit voltage can be as large as  $-4.0$  V (vs. Al) (Fig. 5), which is adequate to allow the electrochemical extraction of Nd. A pair of redox peaks ( $p, p'$ ) appear after the addition of a calculated amount of  $\text{LiCF}_3\text{SO}_3$  into EC. However, there is no reduction signal before lithium reduction ( $-2.68$  V vs. Al), demonstrating excellent electrochemical performance of the Li-containing supporting electrolyte.

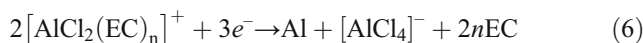
No other electrochemical signals can be observed after “ $b_1$ ” in the CV curve of EC/ $\text{AlCl}_3$  (2:1, mole ratio) shown in Fig. 6 (red line), indicating that there is no electrochemical reaction related to this solvent. Therefore, combine the above CV analysis of EC/ $\text{LiCF}_3\text{SO}_3$  system, this Al-containing system is electrochemically stable and can be used for electrodeposition of other active metals and alloys from the corresponding soluble precursors.

A pair of redox peaks ( $a, a'$ ) appears after the addition of a calculated amount of  $\text{NdCl}_3$  into the EC/ $\text{AlCl}_3$  (2:1, mole ratio) system (Fig. 6, black line), which correspond to the

oxidation and reduction process of the metallic Nd on the tungsten working electrode, respectively. Based on previous studies [19], the reduction process of Nd should be a direct one-step process (Eq. 5):



Notably, similar to the EC/ $\text{AlCl}_3$  (2:1, mole ratio) system, there is a reduction signal, denoted “ $b_2$ ,” observed before the precipitation of metallic Nd. This should be ascribed to the discharge process of Al-containing cations  $[\text{AlCl}_2(\text{EC})_n]^+$ . Al can be reduced in one step, gaining electrons through the following pathway (Eq. 6) [34]:



As is known, the electrodeposition of Al in traditional first-generation ILs has been widely reported over the past few decades. It is generally believed that Lewis acid anions  $[\text{Al}_2\text{Cl}_7]^-$  are the electroactive species in Al electrodeposition. However, as further research is being conducted, especially on the application of chloroaluminate IL-like systems in Al secondary batteries, more and more studies have testified that Al can be electrodeposited from Al-containing cations [39–41]. Therefore, if the Al-containing cations were eliminated, then the single metal Nd could be electrodeposited. Such studies are currently in progress. In addition, compared with the conventional  $\text{AlCl}_3$ –EMICl IL system for the deposition of Al or alloys, the advantages of EC/ $\text{AlCl}_3$  electrolyte include facile preparation, water insensitive [34], and good electrochemical stability.

The characterization of the electrodeposited materials by XRD confirmed that an Al–Nd alloy can be obtained in the form of  $\text{Al}_2\text{Nd}$  (PDF#00-029-0054) by electrochemical codeposition at higher cathode overpotential ( $-3.5$  V vs. Al) during a 3-h potentiostatic electrolysis (Fig. 7). No EC was consumed or deteriorated during electrodeposition, which is an example of green metallurgy using a green solvent.

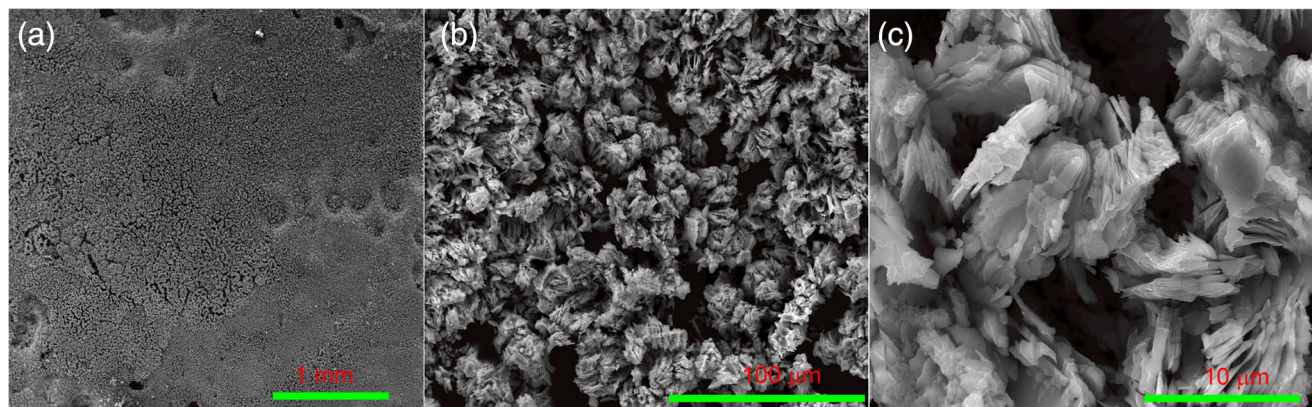


**Fig. 8** SEM images of the material deposited on the Al substrate at **a**  $\times 80$ , **b**  $\times 1300$ , and **c**  $\times 10,000$  magnification

The reason for the formation of  $\text{Al}_2\text{Nd}$  compounds is that the deposited Nd can alloy with pre-deposition reactive Al or the Al cathode plate, and the thermally stable Al-Nd intermetallic compounds are relatively easy to form because of the large difference in electronegativity between Al and Nd. In the field of Al-based Nd alloy materials,  $\text{Al}_2\text{Nd}$  is the main strengthening phase [3]. Hence, the codeposition of Al and Nd ions in this IL provides a unique opportunity for the preparation of Al-Nd alloys in one step near room temperature, which can save energy and achieve cost-competitive production.

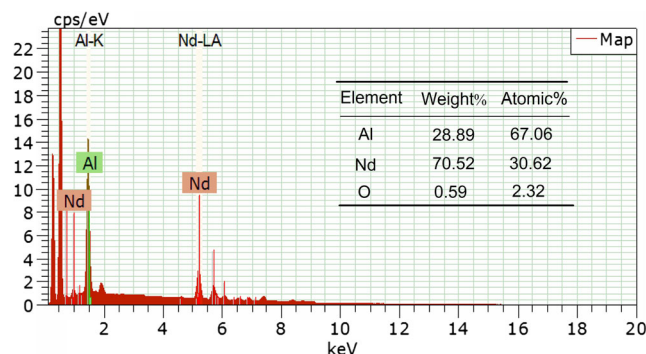
### Surface morphology of Al-Nd alloy

Figure 8 shows the SEM images of the surface morphology of the Al-Nd alloy layer electrodeposited on an Al substrate. As a whole, the quality of the alloy layer is loose, not dense (Fig. 8a). The processes governing metal grain nucleation and growth seem to be complicated (Fig. 8b); a twisted stratiform alloy is observed at high magnification (Fig. 8c). The porosities of the materials deposited on Al substrates are given in Table 1, directly indicating the porous and uncompacted properties of the deposited coatings, which is in accordance with the SEM-visualized surface morphology. Moreover, the average porosity of these samples is about 38.4%. Furthermore, it should be noted that the deposit is non-uniform with some bald spots present in some cases. Based on this observation, we are able to change the electrolysis conditions, such as current density, overpotential, and time, to improve the appearance of the deposited material. Although there are some visible defects in the deposited material, from the electrochemical metallurgy point of view, low-temperature electrodeposition of Al-Nd alloy is proven to be feasible in this stable solvate IL. Figure 9 presents the corresponding EDX spectrum and elemental composition of the material electrodeposited on an Al substrate observed in Fig. 8a. All the EDX spectra only consist of the strong peak of Al and Nd which indicates that the main constituent is Al and Nd. The atomic percentage content confirms the existence of  $\text{Al}_2\text{Nd}$  alloy, which echoes the XRD results.

In addition, we could control the composition and apparent morphology of the alloy by regulating the molar ratio of  $\text{AlCl}_3/\text{NdCl}_3$ . Accordingly, Al-containing solvate ILs, which to an extent evolved from ILs and IL-like systems, are of increasing interest. They are expected to gain more attention

**Table 1** Total porosity of the samples obtained on four Al substrates during 3-h potentiostatic electrolysis at  $-3.5$  V vs. Al

| Sample no. | Total porosity |
|------------|----------------|
| 01#        | 40.5%          |
| 02#        | 42.6%          |
| 03#        | 36.8%          |
| 04#        | 33.7%          |



**Fig. 9** EDX spectrum and elemental composition of the material observed in Fig. 8a

in the field of green electrochemical metallurgy due to their tunable Lewis acidity and lower price.

### Conclusions

In this work, an Al-containing solvate IL was formed between the O-donor EC and Lewis-acidic  $\text{AlCl}_3$  at a molar ratio of 2:1 and used for dissolving  $\text{NdCl}_3$ ; this mixture was then used for the electrochemical deposition of an Al-Nd alloy near room temperature (323 K). The differences between the first generation IL ( $\text{AlCl}_3\text{-EMICl}$ ) and this solvate IL are discussed and analyzed in relation to the dissolution mechanism of  $\text{NdCl}_3$ , and the dissolution mechanism of  $\text{NdCl}_3$  in  $\text{EC}/\text{AlCl}_3$  (2:1, mole ratio) solvate IL was derived to be:  $3[\text{AlCl}_2(\text{EC})_n]^+ + 2\text{NdCl}_3 \rightleftharpoons 2\text{Nd(III)} + 3[\text{AlCl}_4]^- + 3n\text{EC}$ . An Al-Nd alloy can be obtained in the form of the thermally stable  $\text{Al}_2\text{Nd}$  phase by electrochemical codeposition. Cyclic voltammetry shows that the electrodeposition of Nd is a direct one-step process, and the electrodeposition of Al originates from the Al-containing cations  $[\text{AlCl}_2(\text{EC})_n]^+$ . Although the surface appearance of the electrodeposited material is not very dense, it is a promising result for enabling green electrochemical enrichment and making electrometallurgy more energy-efficient and environmentally friendly.

**Funding information** This work was financially supported by the National Key R&D Program of China (No. 2017YFC0805100), National Natural Science Foundation of China (No. 51574071), and the Fundamental Research Funds for the Central Universities (N172502003).

### References

- Song X, Zhang J, Yue M, Li E, Zeng H, Lu N, Zhou M, Zuo T (2006) Technique for preparing ultrafine nanocrystalline bulk material of pure rare-earth metals. *Adv Mater* 18(9):1210–1215
- Kanna RR, Sakthipandi K, Maraikkayar SMSMA, Lenin N, Sivabharathy M (2018) Doping effect of rare-earth (lanthanum, neodymium and gadolinium) ions on structural, optical, dielectric and magnetic properties of copper nanoferrites. *J Rare Earths* 36(12):1299–1309

3. Su M, Zhang J, Feng Y, Bai Y, Wang W, Zhang Z, Jiang F (2017) Al-Nd intermetallic phase stability and its effects on mechanical properties and corrosion resistance of HPDC Mg-4Al-4Nd-0.2Mn alloy. *J Alloys Compd* 691:634–643
4. Cao ZJ, Kong G, Che CS, Wang YQ, Peng HT (2017) Experimental investigation of eutectic point in Al-rich Al-La, Al-Ce, Al-Pr and Al-Nd systems. *J Rare Earths* 35(10):1022–1028
5. Gu Y, Liu J, Qu S, Deng Y, Han X, Hu W, Zhong C (2017) Electrodeposition of alloys and compounds from high-temperature molten salts. *J Alloys Compd* 690:228–238
6. Liu F, Deng Y, Han X, Hu W, Zhong C (2016) Electrodeposition of metals and alloys from ionic liquids. *J Alloys Compd* 654:163–170
7. Abbott AP, McKenzie KJ (2006) Application of ionic liquids to the electrodeposition of metals. *Phys Chem Chem Phys* 8(37):4265–4279
8. Lisenkov A, Zheludkevich ML, Ferreira MGS (2010) Active protective Al-Ce alloy coating electrodeposited from ionic liquid. *Electrochem Commun* 12(6):729–732
9. Bourbos E, Giannopoulou I, Karantonis A, Paspaliaris I, Papias D (2018) Reduction of light rare earths and a proposed process for Nd electrorecovery based on ionic liquids. *J Sustain Metall* 4(3):395–406
10. Shen D, Akolkar R (2017) Electrodeposition of neodymium from NdCl<sub>3</sub>-containing eutectic LiCl-KCl melts investigated using voltammetry and diffusion-reaction modeling. *J Electrochem Soc* 164(8):H5292–H5298
11. Hua ZS, Liu H, Wang J, He J, Xiao SJ, Xiao YP, Yang YX (2017) Electrochemical behavior of neodymium and formation of Mg-Nd alloys in molten chlorides. *ACS Sustain Chem Eng* 5(9):8089–8096
12. Tang H, Pestic B (2015) Electrochemistry and the mechanisms of nucleation and growth of neodymium during electroreduction from LiCl-KCl eutectic salts on Mo substrate. *J Nucl Mater* 458:37–44
13. Liu K, Liu YL, Chai ZF, Shi WQ (2017) Evaluation of the electroextractions of Ce and Nd from LiCl-KCl molten salt using liquid Ga electrode. *J Electrochem Soc* 164(4):D169–D178
14. Simka W, Puszczyc D, Nawrat G (2009) Electrodeposition of metals from non-aqueous solutions. *Electrochim Acta* 54(23):5307–5319
15. Welton T (2018) Ionic liquids: a brief history. *Biophys Rev Lett* 10(3):691–706
16. Hallett JP, Welton T (2011) Room-temperature ionic liquids: solvents for synthesis and catalysis. *Chem Rev* 111(5):3508–3576
17. Haarberg GM (2018) Challenges for electrochemical research in molten salts and ionic liquids. *Electrochemistry* 86(2):19
18. Chou LH, Hussey CL (2014) An electrochemical and spectroscopic study of Nd (III) and Pr (III) coordination in the 1-Butyl-1-methylpyrrolidinium bis (trifluoromethylsulfonyl) imide ionic liquid containing chloride ion. *Inorg Chem* 53(11):5750–5758
19. Bagria P, Luo H, Popovsa I, Thapaliyac BP, Dehautda J, Dai S (2018) Trimethyl phosphate based neutral ligand room temperature ionic liquids for electrodeposition of rare earth elements. *Electrochem Commun* 96:88–92
20. Kondo H, Matsumiya M, Tsunashima K, Kodama S (2012) Attempts to the electrodeposition of Nd from ionic liquids at elevated temperatures. *Electrochim Acta* 66:313–319
21. Ota H, Matsumiya M, Sasaya N, Nishihata K, Tsunashima K (2016) Investigation of electrodeposition behavior for Nd (III) in [P2225][TFSA] ionic liquid by EQCM methods with elevated temperatures. *Electrochim Acta* 222:20–26
22. Matsumiya M, Mai I, Kazama R, Kawakami S (2014) Electrochemical analyses of diffusion behaviors and nucleation mechanisms for neodymium complexes in [DEME][TFSA] ionic liquid. *Electrochim Acta* 146:371–377
23. Smith EL, Abbott AP, Ryder KS (2014) Deep eutectic solvents (DESSs) and their applications. *Chem Rev* 114(21):11060–11082
24. Abbott AP, Boothby D, Capper G, Davies DL, Rasheed RK (2004) Deep eutectic solvents formed between choline chloride and carboxylic acids: versatile alternatives to ionic liquids. *J Am Chem Soc* 126(29):9142–9147
25. Coleman F, Srinivasan G, Swadzba-Kwasny M (2013) Liquid coordination complexes formed by the heterolytic cleavage of metal halides. *Angew Chem Int Ed* 52(48):12582–12586
26. Hogg JM, Coleman F, Ferrer-Ugalde A, Atkins MP, Swadzba-Kwasny M (2015) Liquid coordination complexes: a new class of Lewis acids as safer alternatives to BF<sub>3</sub> in synthesis of polyalphaolefins. *Green Chem* 17(3):1831–1841
27. Abbott AP, Harris RC, Hsieh YT, Ryder KS, Sun IW (2014) Aluminium electrodeposition under ambient conditions. *Phys Chem Chem Phys* 16(28):14675–14681
28. Abbott AP, Capper G, Davies DL (2006) Solubility of metal oxides in deep eutectic solvents based on choline chloride. *J Chem Eng Data* 51(4):1280–1282
29. Fang Y, Yoshii K, Jiang X, Sun XG, Tsuda T, Mehio N, Dai S (2015) An AlCl<sub>3</sub> based ionic liquid with a neutral substituted pyridine ligand for electrochemical deposition of aluminum. *Electrochim Acta* 160:82–88
30. Fang Y, Jiang X, Sun XG, Dai S (2015) New ionic liquids based on the complexation of dipropyl sulfide and AlCl<sub>3</sub> for electrodeposition of aluminum. *Chem Commun* 51(68):13286–13289
31. Abood HM, Abbott AP, Ballantyne AD, Ryder KS (2011) Do all ionic liquids need organic cations? Characterisation of [AlCl<sub>2</sub>-nAmide]<sup>+</sup> AlCl<sub>4</sub><sup>-</sup> and comparison with imidazolium based systems. *Chem Commun* 47(12):3523–3525
32. Li M, Gao B, Liu C, Chen W, Wang Z, Shi Z, Hu X (2017) AlCl<sub>3</sub>/amide ionic liquids for electrodeposition of aluminum. *J Solid State Electrochem* 21(2):469–476
33. Abedin SZE (2012) Electrochemical behavior of aluminum and some of its alloys in chloroaluminate ionic liquids: electrolytic extraction and electrorefining. *J Solid State Electrochem* 16(2):775–783
34. Zhang BG, Shi ZN, Shen LL, Liu AM, Xu JL, Hu XW (2018) Electrodeposition of Al, Al-Li alloy, and Li from an Al-containing solvate ionic liquid under ambient conditions. *J Electrochem Soc* 165(9):D321–D327
35. Zhang BG, Yao Y, Shi ZN, Xu JL, Wang ZW (2018) Direct electrochemical deposition of lithium from lithium oxide in a highly stable aluminium-containing solvate ionic liquid. *ChemElectroChem* 5(22):3368–3372
36. Hu P, Zhang R, Meng X, Liu H, Xu C, Liu Z (2016) Structural and spectroscopic characterizations of amide-AlCl<sub>3</sub>-based ionic liquid analogues. *Inorg Chem* 55(5):2374–2380
37. Tsuda T, Nohira T, Ito Y (2001) Electrodeposition of lanthanum in lanthanum chloride saturated AlCl<sub>3</sub>-1-ethyl-3-methylimidazolium chloride molten salts. *Electrochim Acta* 46(12):1891–1897
38. Brown LC, Hogg JM, Swadzba-Kwasny M (2017) Lewis acidic ionic liquids. *Top Curr Chem* 375(5):78–85
39. Li JF, Tu JG, Jiao HD, Wang C, Jiao SQ (2017) Ternary AlCl<sub>3</sub>-urea-[EMIm] Cl ionic liquid electrolyte for rechargeable aluminum-ion batteries. *J Electrochem Soc* 164(13):A3093–A3100
40. Zhang C, Yu D, Zhang L, Wang X, Zhao Y, Zhang X, Yu G (2017) A sustainable redox-flow battery with an aluminum-based deep-eutectic-solvent anolyte. *Angew Chem Int Ed* 56(26):7454–7459
41. Mutlu RN, Yazıcı B (2019) Copper-deposited aluminum anode for aluminum-air battery. *J Solid State Electrochem* 23(2):529–541